Talanta ∎ (∎∎∎∎) ∎∎∎–∎∎∎

Contents lists available at SciVerse ScienceDirect

Talanta

journal homepage: www.elsevier.com/locate/talanta

New fluorescent pH sensors based on covalently linkable PET rhodamines

Daniel Aigner [a], Sergey M. Borisov [a,*], Francisco J. Orriach Fernández [b], Jorge F. Fernández Sánchez [b], Robert Saf [c], Ingo Klimant [a]

[a] Institute of Analytical Chemistry and Food Chemistry, Graz University of Technology, Stremayrgasse 9, A-8010 Graz, Austria
[b] Department of Analytical Chemistry, University of Granada, Avd. Fuentenueva s/n, E-18071 Granada, Spain
[c] Institute for Chemistry and Technology of Materials, Graz University of Technology, Stremayrgasse 9, A-8010 Graz, Austria

ARTICLE INFO

Article history:
Received 26 January 2012
Received in revised form
18 May 2012
Accepted 19 May 2012

Keywords:
pH sensor
Fluorescence
Rhodamine
Photoinduced electron transfer
Covalent dye coupling
"Click" chemistry

ABSTRACT

A new class of rhodamines for the application as indicator dyes in fluorescent pH sensors is presented. Their pH-sensitivity derives from photoinduced electron transfer between non-protonated amino groups and the excited chromophore which results in effective fluorescence quenching at increasing pH. The new indicator class carries a pentafluorophenyl group at the 9-position of the xanthene core where other rhodamines bear 2-carboxyphenyl substituents instead. The pentafluorophenyl group is used for covalent coupling to sensor matrices by "click" reaction with mercapto groups. Photophysical properties are similar to "classical" rhodamines carrying 2′-carboxy groups. pH sensors have been prepared with two different matrix materials, silica gel and poly(2-hydroxyethylmethacrylate). Both sensors show high luminescence brightness (absolute fluorescence quantum yield $\Phi_F \approx 0.6$) and high pH-sensitivity at pH 5–7 which makes them suitable for monitoring biotechnological samples. To underline practical applicability, a dually lifetime referenced sensor containing Cr(III)-doped Al_2O_3 as reference material is presented.

1. Introduction

pH is a key parameter for a wide range of applications in the medical field, in environmental and life sciences or for regulation and routine monitoring in industrial processes and in sewage purification plants, to mention only a few areas. Although electrochemical pH sensors are well-established and can be used as reliable tools for a large number of analytical tasks, optical pH sensors offer unmatched advantages in many other challenging applications, in particular for high-throughput screening, for applications where minimal contact to the sample is preferable, where a high degree of miniaturisation is required or in systems that do not allow the application of potentiometric sensors due to a strong electromagnetic field.

A number of fluorescent pH sensors have already been established in which derivatives of 8-hydroxypyrene-1,3,6-trisulfonate (HPTS) [1–3], fluoresceins [4–7] and benzo[g]xanthene dyes [8–10] have been the most common pH-sensitive indicator dyes. Most of these indicators, however, still are subject to limitations. Fluoresceins are commonly known for their limited photostability. HPTS derivatives are excitable at relatively short (< 500 nm) wavelengths which results in high levels of autofluorescence and scattering background. Benzo[g]xanthene dyes are long-wave excitable, but offer only limited brightness (defined as the product of molar absorption coefficient ε and fluorescence quantum yield, Φ_F) $\leq 12 \times 10^3$ M^{-1} cm^{-1} [8], which is at least 5 times lower than for the dyes presented in this work, and are prone to photobleaching [11].

Rhodamines are xanthene dyes featuring outstanding brightness (high ε about 1×10^5 M^{-1} cm^{-1} and Φ_F of 0.7–1 for most derivatives), generally good solubility in water and good photostability [12]. These properties have enabled their application in cell imaging [13,14] and single molecule imaging [15,16], for the characterisation of micelles [17] and polymer beads [18], as standards for fluorescence quantum yield [19] or as molecular switches [16,20] and fluorescence thermometers [21], to state only a few. Numerous rhodamine-based fluorescent probes for cations–most importantly Hg^{2+} [14,22,23], Cu^{2+} [24,25], Fe^{3+} [26], Pb^{2+} [27]– and thiols [28] have been presented. On the other hand pH-sensitive systems relying on rhodamines as pH probes [29–36] are less common. Since most of these systems take advantage of the cyclisation equilibrium in rhodamines leading to non-fluorescent spyro-lactams we believe that alternative concepts for designing pH indicators on the basis of rhodamine dyes are of high interest.

Here we present a new class of amino-functional rhodamines the pH-sensitivity of which originates from the intramolecular photoinduced electron transfer process (PET, [37–42]) between

* Corresponding author. Tel.: +43 316 87332516; fax.: +43 316 87332502.
E-mail address: sergey.borisov@tugraz.at (S.M. Borisov).

0039-9140/$ - see front matter © 2012 Elsevier B.V. All rights reserved.
http://dx.doi.org/10.1016/j.talanta.2012.05.039

non-protonated amino groups and the excited chromophore (Fig. 1). To the best of our knowledge, only very few examples for pH-sensitive PET rhodamines [43,44] can be found in the literature and those focus on application as probes in solution, not in a solid sensor matrix. The new dye class is accessible by a straightforward one-step synthesis. It carries a pentafluorophenyl group in the 9-position of the xanthene core which is employed for simple and effective covalent coupling by "click" reaction with mercapto groups. Covalent indicator linkage can be highly beneficial for pH optrodes since it suppresses migration and aggregation processes. Nucleophilic substitution in pentafluorophenyl groups has recently been presented as a versatile tool for grafting [45–49]. The suitability of the new fluorinated PET-rhodamines as indicators in pH sensors will be demonstrated.

2. Experimental

2.1. Materials and methods

3-(1-Piperazinyl)phenol, pentafluorobenzaldehyde, methanesulfonic acid and (3-mercaptopropyl)trimethoxysilane were purchased from ABCR (www.abcr.de). Urea was from Acros (www.acros.com). All other reagents were obtained from Aldrich (www.sigmaaldrich.com). All reagents were of synthesis grade. Deuterated solvents were purchased form eurisotop (www.eurisotop.com). Anhydrous pydridine and *N*,*N*-dimethylformamide were bought from Aldrich. All other solvents (synthesis grade, HPLC gradient grade), as well as potassium persulfate, sodium chloride and buffer salts, were supplied by Carl Roth (www.carlroth.de). Hydroxyethylmethacrylate and ethylene glycol dimethacrylate were filtered over aluminium oxide prior to use. Water used for HPLC chromatography was deionised using a Barnstedt NANOpure system. Dowex® 1–8 cation exchange resin was freshly charged with chloride prior to use.

Absorption measurements were performed on a Cary 50 UV–vis spectrophotometer from Varian (www.varianinc.com). Fluorescence spectra were recorded on a Hitachi F-7000 spectrofluorimeter (www.hitachi.com). Relative fluorescence quantum yields Φ_F were determined using rhodamine 101 (Φ_F=0.96 [50]; Fluka, www.sigmaaldrich.com) as a standard. Absolute fluorescence quantum yields were determined on a Fluorolog 3 spectrofluorimeter equipped with an integrating sphere (Horiba Scientific, www.horiba.com). ^{1}H-NMR spectra were recorded on a 300 MHz instrument (Bruker) with TMS as a standard. ^{19}F-NMR spectra were taken on a Mercury Inova 300 instrument (Bruker) at a frequency of 282.47 MHz. MALDI-TOF masses were determined on a Micromass TofSpec 2E in reflectron mode at an accelerating voltage of +20 kV. pH calibration curves and sensor response curves were obtained by passing buffer solutions (1 ml min^{-1}) by a sensor foil placed in a home-made flow-through cell. Cell temperature was kept constant at 25 °C. The luminescent signal was interrogated with a two-phase lock-in amplifier (SR830, Stanford Research Inc., www.thinksrs.com) equipped with a green LED (λ_{max} 525 nm) from Roithner (www.roithner-laser.com), a XR3080 bandpass filter (500–540 nm; Horiba, www.horiba.com) at the excitation side and a long-pass filter (Schott, www.schott.com; OG 580 (> 580 nm), unless otherwise stated) before the PMT tube (H5701-02, Hamamatsu, www.

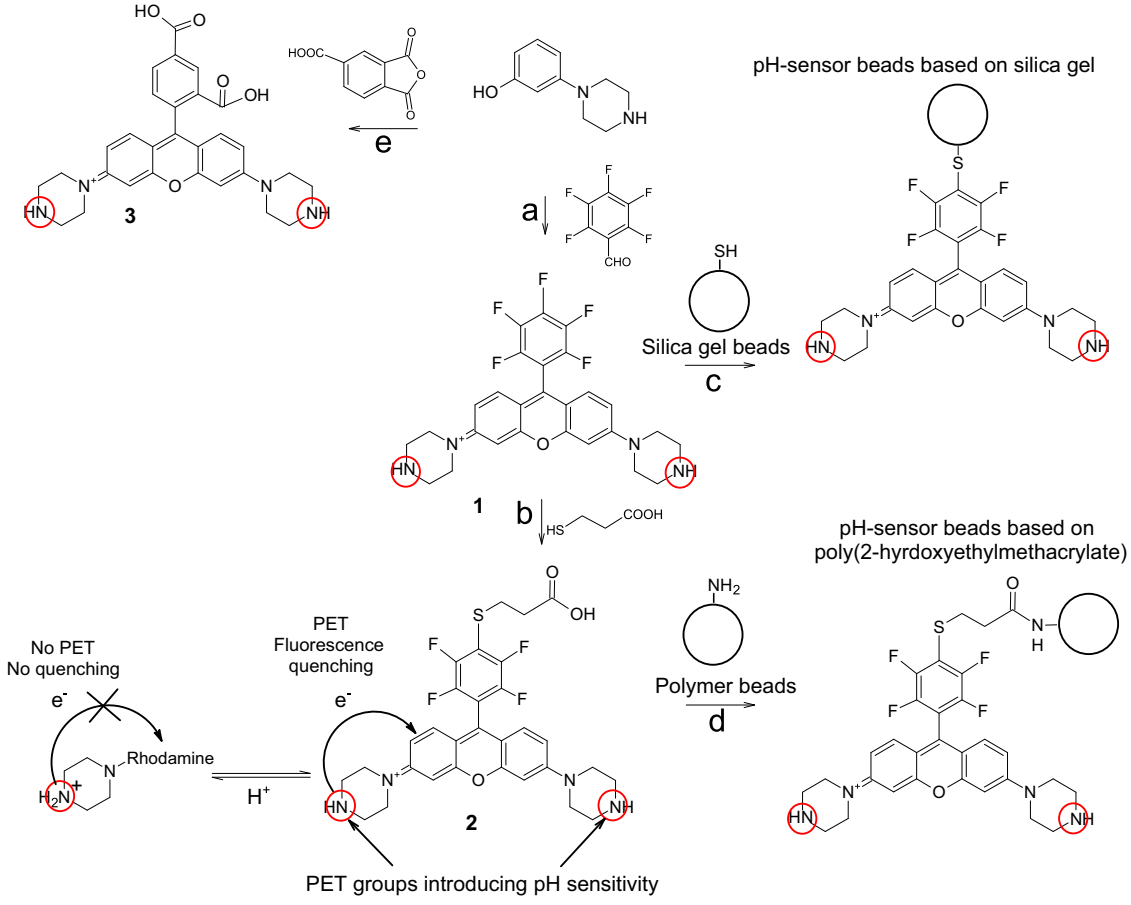

Fig. 1. Preparation of the pH-indicators **1–3** and the two types of pH-sensor beads. Reagents and conditions: (a) pentafluorobenzaldehyde, CH_3SO_3H, 210 °C (28%); (b) 3-mercaptopropionic acid, Et_3N, *N*,*N*′-dimethylacetamide, 50 °C (39%); (c) mercapto-functionalised silica gel beads, Et_3N, *N*,*N*′-dimethylacetamide, 60 °C; (d) amino-functionalised poly(HEMA) beads, DCC, NHS, DMAP, *N*,*N*′-dimethylformamide; and (e) trimellitic anhydride, CH_3SO_3H, 165 °C (21%).

Please cite this article as: D. Aigner, et al., New fluorescent pH sensors based on covalently linkable PET rhodamines, Talanta (2012), http://dx.doi.org/10.1016/j.talanta.2012.05.039

sales.hamamatsu.com). The modulation frequency of 160 Hz was used, unless otherwise stated. The pH of the phosphate and acetate buffer solutions was controlled by a digital pH metre (InoLab pH/ion, WTW GmbH & Co. KG, www.wtw.com) calibrated at 25 °C with standard buffers of pH 7.0 and 4.0 (WTW GmbH & Co. KG, www.wtw.com). The buffers were adjusted to constant ionic strength using sodium chloride as a background electrolyte. LCMS measurements were performed on a Shimadzu LCMS system equipped with a LSMS-2020 mass detector and a SPD-M20A diode array detector (www.shimadzu.de).

2.2. Preparation of dyes and sensors

N,*N*′-di(3-azapentane-1,5-diyl)-2′,3′,4′,5′,6′-pentafluororhodamine acetate (**1**)

A mixture of 3-(1-piperazinyl)phenol (2.7 g, 15.15 mmol), pentafluorobenzaldehyde (1.5 g, 7.65 mmol) and methanesulfonic acid (20 ml) was heated to 210 °C under vigorous stirring. Temperature was maintained for 4.5 h, pentafluorobenzaldehyde (500 mg, 2.5 mmol) was added in two equal portions during the first 2.5 h. The deep red mixture was allowed to cool to RT and was added dropwise into THF (250 ml). The sticky solid formed was redissolved in MeOH (50 ml) and again precipitated with THF (250 ml). The procedure was repeated six times until a black powder was obtained. The powder was dissolved in H_2O (100 ml) and passed over Dowex® 1–8 cation exchange resin (Carl Roth) charged with chloride. The deep red solution was dried to yield 3.8 g of crude product. Purification was performed by HPLC chromatography on an Agilent 1100 station (www.chem.agilent.com) employing a Nucleodor 100–5 μm C18ec reversed phase column (Macherey Nagel; 200 × 15 mm) and MeOH/0.1% aqueous acetic acid (gradient is stated in Table S1) as the mobile phase. Upon purification, 37 mg crude product yielded 12 mg pure **1.** Owing to the limited size of the available HPLC facility, not all crude **1** was purified. If up-scaling is performed, 1.23 g (2.14 mmol, 28%) of pure **1** can be isolated. ^{1}H NMR (300 MHz, CD_3OD containing 0.1% HOAc and 0.1% CF_3COOH, TMS): δ=7.65 ppm (2H, d, Ar-H(positions 1,8), $J_{ArH12,78}$=9.6 Hz); δ=7.46 (2H, dd, Ar-H(2,7), $J_{ArH24,57}$=2.5 Hz); δ=7.42 (2H, d, Ar-H(4,5)); δ=4.13 (8H, t, $ArNCH_2$, J=5.2 Hz); δ=3.48 (8H, t, $HNCH_2$); δ=1.99 (3H, s, $H_{acetate}$). ^{19}F-NMR (282.5 MHz, D_2O): δ=−139 ppm (2F, d, J=20 Hz); δ=−150 (1F, t, J=21 Hz); δ=−160 (2F, dt, J_1=6 Hz, J_2=21 Hz). MALDI-TOF: m/z [MH^+] 515.1847 found, 515.1870 calcd.

N,*N*′-di(3-azapentane-1,5-diyl)-4′-(2-carboxyethylmercapto)-2′,3′,5′,6′-tetrafluororhodamine acetate (**2**)

Crude **1** (328 mg, containing 157 mg, 278 μmol of pure **1**[1]), *N*,*N*-dimethylacetamide (8 ml) and triethylamine (248 μl, 1.78 μmol) were heated to 50 °C and 3-mercaptopropionic acid (34.4 μl, 390 μmol) was added dropwise. Temperature was maintained for 3 h and the mixture was washed with hexane until a solid residue was obtained (4 × 100 ml). The residue was dissolved in MeOH/1 M aqueous HCl 1:1 (3 × 10 ml) and precipitated with THF (3 × 150 ml). Crude **2** was obtained as a black powder (130 mg). Purification was performed similarly to **1** (different gradient is stated in table S2) and yielded 19 mg of pure **2** (35 mg crude product; 71 mg (0.11 mmol, 39%) if up-scaled). ^{1}H NMR (300 MHz, CD_3OD containing 0.1% CF_3COOH, TMS): δ=7.55 ppm (2H, d, Ar-H(positions 1,8), $J_{ArH12,78}$=9.6 Hz); δ=7.32 (2H, dd, Ar-H(2,7), $J_{ArH24,57}$=2.3 Hz); δ=7.26 (2H, d, Ar-H(4,5)); δ=4.06 (8H, t, $ArNCH_2$, J=4.9 Hz); δ=3.48 (8H, t, $HNCH_2$); δ=3.32 (2H, t, $ArSCH_2$, J=6.7 Hz); δ=2.76 (2H, t, CH_2COOH); δ=2.06 (4.7H, s, $H_{acetate}$). ^{19}F-NMR (282.5 MHz, D_2O): δ=−132 ppm (2F, q, J=11 Hz); δ=−139 (2F, q, J=11 Hz). MALDI-TOF: m/z [MH^+] 601.1923 found, 601.1896 calcd.

N,*N*′-di(3-azapentane-1,5-diyl)-2′,4′-dicarboxyrhodamine acetate (**3**)

Trimellitic anhydride (1.62 g, 8.42 mmol), 3-(1-piperazinyl)-phenol (3 g, 16.83 mmol) and methanesulfonic acid (25 ml) were heated to 165 °C. Temperature was maintained for 3.5 h, the deep red mixture was allowed to cool to RT and was added dropwise into THF (100 ml). The sticky black precipitate was redissolved in MeOH and precipitated by adding THF. The procedure was repeated six times to yield crude **3** (1.8 g) as a black powder. Purification was performed similarly to **1** (different gradient is stated in Table S3) and yielded 14 mg of pure **3** (44 mg crude product; 890 mg (1.74 mmol, 21%) if up-scaled). Both the 4′-carboxy and the 5′-carboxy regioisomer could be isolated in pure form and identified by NMR spectroscopy (Figs. S9 and S10). Although the 5′-carboxy isomer was formed in comparable amounts (Fig. S18) and is equally suitable for the present application, only pure 4′-carboxy isomer was used for characterisation. ^{1}H NMR (300 MHz, D_2O, TMS): δ=8.32 ppm (1H, s, Ar-H(position 3′)); δ=8.00 ppm (1H, d, Ar-H(5′), $J_{ArH5'6'}$=7.5 Hz); δ=7.27 (3H, d, Ar-H(6′,1,8), $J_{ArH12,78}$=9.3 Hz); δ=7.06 (2H, d, Ar-H(2,7)); δ=6.97 (2H, s, Ar-H(4,5)); δ=3.85 (8H, broad s, $ArNCH_2$); δ=3.35 (8H, broad s, $HNCH_2$); δ=1.90 (3H, s, $H_{acetate}$). MALDI-TOF: m/z [MH^+] 513.2101 found, 513.2138 calcd.

2.3. Mercapto-functionalised silica gel beads

Li Chrospher 60 silica gel beads (Merck, average size 5 μm; 1 g) were dispersed in EtOH/H_2O 19:1 (40 ml) in a polypropylene vessel. (3-Mercaptopropyl)trimethoxysilane (26.8 μl, 0.144 mmol) and acetic acid (2 ml) were added and the mixture was stirred overnight at RT. The beads were separated by centrifugation (2450 g), washed with EtOH (6 × 50 ml) and dried (60 °C, 1 bar).

2.4. Amino-functionalised poly(hydroxyethylmethacrylate) (poly(HEMA)) beads

Poly(HEMA) beads were prepared adapting a method reported in the literature [51]. Poly(vinyl alcohol) (86,000 g mol^{-1}, 99% hydrolysed) (3 g) was dissolved in refluxing H_2O (300 ml). The mixture was allowed to cool to 40 °C and flushed with nitrogen for 30 min. 2-Hydroxyethylmethacrylate (3.26 ml, 27.3 mmol), ethylene glycol dimethacrylate (0.36 ml, 1.91 mmol), 2-aminoethylmethacrylate hydrochloride (80 mg, 0.48 mmol) and potassium persulfate (3 mg, 0.01 mmol) were added, the mixture was heated to 70 °C and stirred under a gentle nitrogen stream for 18 h. The precipitated beads were separated by centrifugation (2450 g), washed with H_2O (4 × 100 ml) and EtOH (3 × 100 ml) and freeze-dried (1 mbar, −90 °C, 18 h) to yield 1.6 g of a white powder.

2.5. pH-sensitive silica gel beads

A mixture of mercapto-functionalised silica gel beads (250 mg), rhodamine dye **1** (1 mg, 1.74 μmol), triethylamine (2.7 μl, 0.019 mmol) and *N*,*N*-dimethylacetamide (1 ml) was heated to 60 °C under vigorous stirring for 6 h. The beads were separated by centrifugation (2450 g), washed with 10 mM HCl

[1] Crude **1** was used for the synthesis of **2**. The assay of **1** in the crude product can be easily calculated. The total rhodamine content is equal to the ratio of the molar absorption coefficients of crude and pure product (which is $4.3 \times 10^4\ M^{-1}\ cm^{-1}/8.9 \times 10^4$=0.48). Fig. S13 shows that there are no other rhodamines contained in the crude product (no impurities absorbing at 540 nm). Therefore, the assay of **1** in the crude product is 48% (w/w). For calculation, chloride was the assumed counter ion for crude **1**, while pure **1** is the acetate salt.

Please cite this article as: D. Aigner, et al., New fluorescent pH sensors based on covalently linkable PET rhodamines, Talanta (2012), http://dx.doi.org/10.1016/j.talanta.2012.05.039

(6 × 5 ml), EtOH (2 × 5 ml) and H_2O (6 × 5 ml) and dried (60 °C, 1 bar).

2.6. pH-sensitive poly(HEMA) beads

2 (1 mg, 1.5 μmol) was dissolved in anhydrous *N*,*N*-dimethylformamide (DMF; 0.5 ml) and dicyclohexylcarbodiimide (DCC; 1.37 mg, 6.6 μmol) was added. The solution was stirred at RT for 15 min and N-hydroxysuccinimide (NHS; 1 mg, 8.7 μmol) was added. After 45 min, a dispersion of amino-functionalised poly(HEMA) beads (100 mg) in anhydrous pyridine (1 ml) and a catalytic amount of 4-(dimethylamino)pyridine (DMAP) were added. The mixture was stirred overnight. The beads were separated by centrifugation (2450 g), washed with DMF (2 × 5 ml), CH_2Cl_2 (2 × 5 ml), EtOH (3 × 5 ml), 10 mM HCl (5 × 5 ml) and H_2O (3 × 5 ml) and freeze-dried (1 mbar, −90 °C, 18 h).

2.7. Preparation of Cr(III)-doped Al_2O_3 (ruby)

$Al(NO_3)_3 \cdot 9H_2O$ (16.54 g, 44 mmol), $Cr(NO_3)_3 \cdot 9H_2O$ (0.36 g, 0.90 mmol) and urea (18 g, 0.3 mol) were dissolved in H_2O (100 ml). The mixture was concentrated until a turquoise gel was obtained. The gel was heated to 500 °C and kept at this temperature for 10 min. After cooling to RT, the green solid was ground in a mortar and sintered for 24 h at 1100 °C in air. The pale pink powder obtained was ground in a ball mill to yield 1.9 g of fine Cr-doped Al_2O_3.

2.8. Preparation of the sensor foils

pH-sensitive silica gel beads in D4 hydrogel: A "cocktail" containing silica gel beads (28 mg), hydrogel D4 (41 mg) and EtOH/H_2O 9:1 (500 μl) was knife-coated on a dust-free Mylar support to obtain a sensing layer of about 12.5 μm thickness after solvent evaporation.

pH-sensitive cross-linked poly(HEMA) beads in linear poly(HEMA): Linear poly(HEMA) (MW = 150,000 g mol^{-1}) was dissolved in EtOH:H_2O (9:1 V/V), insoluble residues were separated by centrifugation and discarded. Cross-linked poly(HEMA) beads (10 mg) were added to the obtained solution (29 mg polymer in 500 μl) and the "cocktail" was knife-coated on a dust-free Mylar support to give a sensing layer of about 7 μm thickness after solvent evaporation.

3. Results and discussion

Structures and syntheses of the new pH indicators and sensors are shown in Fig. 1. They are based on **1** which, unlike other rhodamines, does not carry a 2′-carboxy group. For comparison, compound **3** bearing a 2′-carboxy group is also investigated. pH-sensitive rhodamines have been covalently coupled to two different sensor matrices, i.e. silica gel beads and cross-linked poly(2-hydroxyethylmethacrylate) (poly(HEMA)) beads. Polymer hydrogels like poly(HEMA) are the most common matrices in pH sensors. Silica gel represents an interesting alternative material with very different properties. **1** was linked by direct reaction with mercapto-functionalised silica gel beads, while another route involving **2** was employed for the attachment to amino-functionalised poly(HEMA) beads.

3.1. Photophysical properties

The photophysical properties of the synthesised rhodamines and commercially available rhodamine B are displayed in Table 1. The electron-withdrawing highly fluorinated phenyl substituent causes a bathochromic shift of ≈30 nm for both acidic and basic form in compounds **1** and **2** in comparison to **3**. They are therefore excitable at >70 nm longer wavelength than such widely used pH indicators as fluorescein or pyrene derivatives. Luminescence brightness is often expressed as the product of molar absorption coefficient ε and fluorescence quantum yield Φ_F. Both are comparable to the high values known for rhodamines. A somewhat lower Φ_F was found for **1**, while **2** shows almost equal Φ_F to **3** and rhodamine B. Note that mercapto-substituted **2** rather represents the rhodamine structures present in the sensors and is therefore more valid for comparison. Similar Φ_F around 0.6 were found for the presented sensor materials (Table 2). ε are even higher for **1** and **2** than for **3**. Consequently, luminescence brightness of a mercapto-substituted pentafluorophenyl-rhodamine such as **2** is as high as in the case of rhodamines carrying a 2′-carboxy group. Note that in Table 1, lower ε are accompanied by broader

Table 1
Photophysical properties of 1–3 and rhodamine B: absorption maximum (λ_{max} abs) and corresponding molar absorption coefficient (ε); half-width at half maximum in absorption (HWHM); fluorescence emission maximum (λ_{max} em); relative fluorescence quantum yield (Φ_F). Values were determined in aqueous buffer solution, unless otherwise stated. Organic solvents were acidified with CF_3COOH (0.1% V/V) and made basic with Et_3N (0.1% V/V).

Compound	λ_{max} abs (ε 10^{-4})/nm (M^{-1} cm^{-1}) *acidic/basic*	HWHM/nm *acidic/basic*	λ_{max} em/nm acidic	Φ_F *acidic/basic*
1	560(8.82)/584(7.62)	40/57	588	0.40/ < 0.01
2	561(10.2)/583(8.17)	39/54	591	0.67/0.02
3	533(8.46)/554(8.38)	42/43	562	0.69/ < 0.01
Rhodamine B [a]	543(10.6)	35	565	0.70

[a] All values in EtOH, without any acid or base added.

Table 2
Photophysical properties of the sensing materials. The sensor foils were treated with acidic/basic buffer solution, pH 4/9. Prior to measuring Φ_F, the foils were acidified with HCl vapour.

Sensor	λ_{max} exc/nm *acidic/basic*	λ_{max} em/nm *acidic/basic*	Φ_F *acidic*
Silica gel beads in D4 hydrogel	572/583	598/609	0.65
Cross-linked poly(HEMA) beads in linear poly(HEMA)	576/592	601/612	0.61

Please cite this article as: D. Aigner, et al., New fluorescent pH sensors based on covalently linkable PET rhodamines, Talanta (2012), http://dx.doi.org/10.1016/j.talanta.2012.05.039

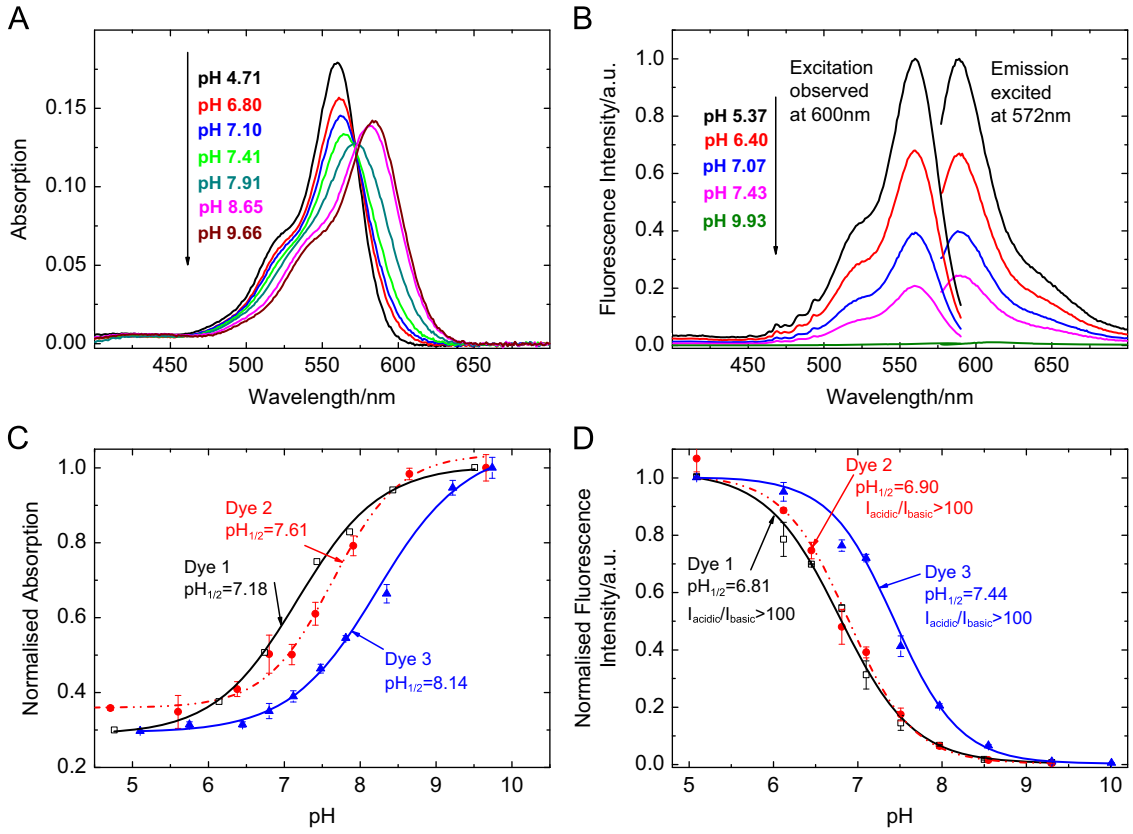

Fig. 2. pH-sensitive properties of **1–3** in aqueous buffer solution (ionic strength 100 mM). Absorption spectra (A) and fluorescence spectra (B) of **2**, dye concentration was 2 μM while recording absorption and 0.05 μM while recording fluorescence spectra. Spectra of **1** and **3** are similar and can be found in the electronic supplementary information. (C) pH calibration curves of **1** (squares), **2** (circles) and **3** (triangles) based on absorption, observed in the absorption maximum of the basic form. (D) Corresponding curves based on fluorescence emission, observed in the emission maximum of the acidic form. $pH_{1/2}$ is the pH at which half of the overall pH-dependent signal change is observed.

absorption peaks (higher half-widths at half maximum, HWHM) so that the integral absorptions of all rhodamines are similar.

3.2. *pH-sensitive properties in aqueous solution*

Absorption and fluorescence spectra of **2** together with pH calibration curves of **1**–**3** are shown in Fig. 2. pH sensitivity is caused by a strong decrease in emission intensity due to photo-induced electron transfer (PET). The sensitive range is around pH=7 so that all dyes are potentially useful for fluorescence imaging in physiological samples. Fluorescence is essentially turned off as deprotonation of the piperazonium groups occurs. A hypsochromic shift of about 20 nm is observed for the absorption spectra of **1**–**3** upon protonation (table 1). This effect is not related to PET. It can be attributed to the electron-withdrawing effect of the positively charged piperazonium groups located in proximity of the rhodamine core. Note that fluorescence spectra are not bathochromically shifted with increasing pH. This indicates that the highly fluorescent acidic form is in equilibrium with a non-fluorescent basic one quenched by PET.

The sensitive range of **1** and **2** (Fig. 2) is found at lower pH than the one of **3**, which illustrates the incomplete decoupling between the piperazinyl groups and the chromophore. The acidic form of **1** and **2** is more strongly destabilised by the vicinity of the rhodamine core that carries a strongly electron-withdrawing fluorinated substituent. Absorption calibration shows response at considerably higher pH than fluorescence calibration. This can be attributed to the fact that shifts in absorption are related to the deprotonation of both piperazonium groups, whereas the deprotonation of the first group may already cause highly efficient PET.

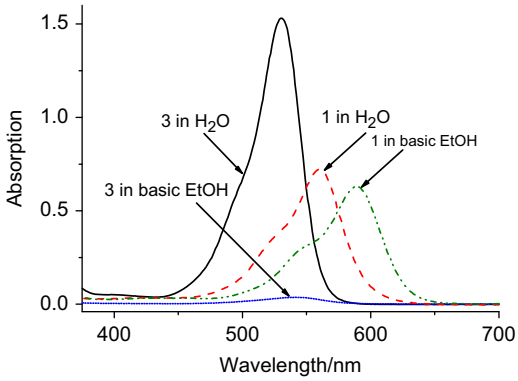

Fig. 3. Lactonisation of **3**, visualised by absorption spectra in H_2O and basic EtOH (containing Et_3N, 0.1% V/V). Due to lactonisation, virtually no absorption is observed in basic EtOH. On the other hand, **1** shows a shift but no attenuation of absorption in basic EtOH compared to H_2O. The slight decrease in the absorption maximum is due to peak broadening, not lactonisation.

Fig. 3 emphasises that **1** does not undergo lactonisation under conditions where **3** is almost completely present in the lactone form. Lactame formation, a very similar process, has been taken advantage of to introduce pH sensitivity into rhodamines [29–34]. In the present system, however, preliminary experiments showed that lactonisation causes almost complete

Please cite this article as: D. Aigner, et al., New fluorescent pH sensors based on covalently linkable PET rhodamines, Talanta (2012), http://dx.doi.org/10.1016/j.talanta.2012.05.039

decolouring of PET rhodamine **3** as soon as it is linked to a sensor matrix. Therefore, the sensors presented in this work rely exclusively on the PET mechanism and employ dyes that do not undergo lactonisation.

3.3. Sensors with covalent dye linkage

Covalent attachment of pH-sensitive rhodamine to both silica gel and cross-linked poly(2-hydroxyethylmethacrylate) (poly (HEMA)) beads was successful, yielding pH sensor beads. For characterisation, the beads were dispersed in polyurethane hydrogel D4® (for the silica gel beads) or in linear poly(HEMA) (for the cross-linked poly(HEMA) beads) to yield planar optrodes. Bright orange fluorescence of the obtained sensors is clearly visible for the acidic form (Fig. 4) and absolute fluorescence quantum yields were found to be rather high (Table 2). Both sensor types exhibit excellent sensitivity and are most useful for measuring pH 5–7 which fits the pH range of interest in many biotechnological applications. The sensors respond at lower pH than the aqueous solutions of **1** and **2**. That is most likely due to the less polar environment in the sensor which destabilises the highly charged acidic form. Förster resonance energy transfer from the acidic to the basic form may also contribute to this effect, since the dye concentration is significantly higher in the sensors than in solution. Despite the high charge of the indicator dye, the sensors show small to moderate cross-sensitivity to ionic strength (Fig. 5). That is particularly true if the ionic strength (IS) is ≥ 100 mM, which is the case in the majority of biotechnological applications. For the silica gel sensors, errors are ≤ 0.1 pH-units if IS= 100–200 mM and ≤ 0.2 pH-units if IS=100–500 mM. They are smaller for the sensor based on poly(HEMA) beads (≤ 0.05 pH-units if IS=100–200 mM and ≤ 0.1 pH-units if IS=100–500 mM), which is expected since poly(HEMA) is a less charged matrix than silica gel [6,52]. The response times are fairly fast ($\tau_{90} < 2$ min for the sensor based on silica gel beads; τ_{90}=2–3 min for the sensor based on poly(HEMA)). Reversibility and repeatability of the sensors are very good, as demonstrated in Fig. 7B and Figs. S3 and S4 in the electronic supplementary information.

Detailed calibration curves are shown in Fig. 4. The silica gel sensor beads are applicable over a broad range (pH 3–8). Measuring at pH > 8 (which is essentially outside the sensitive range) is not recommended and leads to irreversible signal decrease. That is probably caused by hydrolytic cleavage of the Si–O bonds that attach the indicator to the silica gel surface. At pH ≤ 7.5, no signal decrease was observed over many hours. Notably, pH response is broader and quenching at basic pH is less effective than in solution or in the poly(HEMA) beads. This may be related to

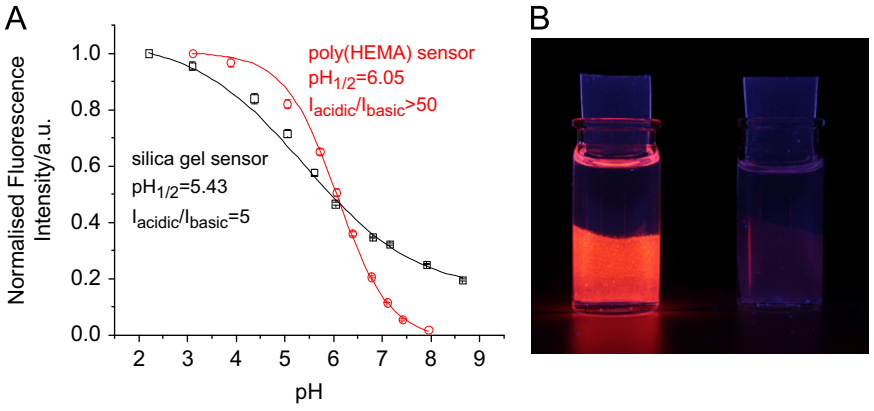

Fig. 4. (A) pH Calibration curves (ionic strength 100 mM) for the sensor foils based on silica gel beads in D4® hydrogel and cross-linked poly(HEMA) beads in linear poly(HEMA), both carrying covalently linked PET rhodamine. $pH_{1/2}$ is the pH at which half of the overall pH-dependent signal change is observed. (B) Photographic image of the poly(HEMA) sensor foils in acidic (pH 4) and basic (pH 9) buffer.

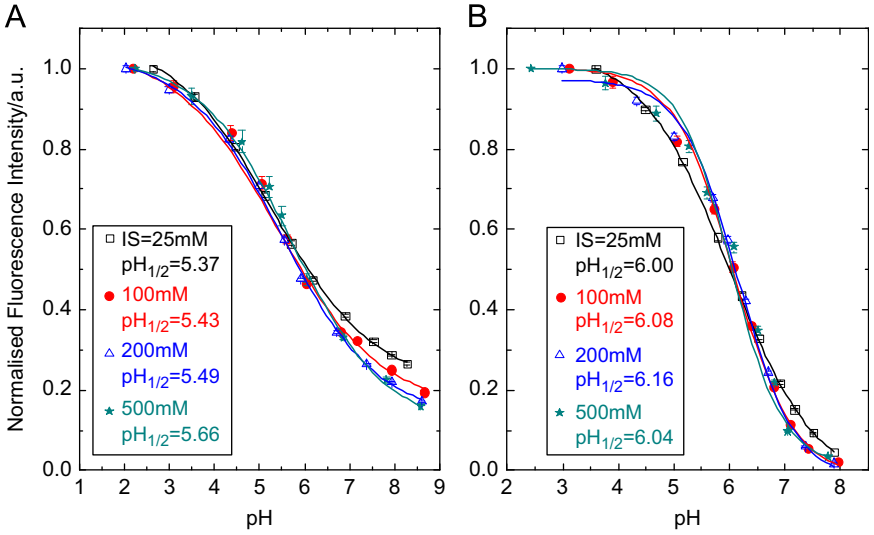

Fig. 5. Calibration curves of the sensor based on silica gel beads (A) and on poly(HEMA) beads (B), measured at different ionic strengths (IS), and corresponding $pH_{1/2}$ values (pH value at which half of the overall pH-dependent signal change is observed).

Please cite this article as: D. Aigner, et al., New fluorescent pH sensors based on covalently linkable PET rhodamines, Talanta (2012), http://dx.doi.org/10.1016/j.talanta.2012.05.039

stabilisation of the cationic acidic form by the negatively charged silica gel surface. Other effects may also contribute to the observed phenomenon. In fact, Gao et al. [53] demonstrated that fluorescence of a rhodamine dye bound to a silica gel surface can be enhanced at increasing pH.

The sensor based on poly(HEMA) beads shows very strong quenching at basic pH and a sharper response at pH 5–7, thus offering excellent sensitivity in this range. It is highly suitable for probing biotechnological samples.

3.4. Photostability

We expected the electron-withdrawing pentafluorophenyl group to suppress photooxidation and therefore improve the photostability of the rhodamines **1** and **2**, compared to **3**. However, the opposite effect was found for **1–3** in aqueous solution (Fig. 6) where **1** and **2** showed measureable photodegradation when illuminated with a high-power 525 nm LED (3 W). This suggests a non-oxidative mechanism as main photodegradation pathway. Therefore, worse photostability can be a drawback in the current system based on pentafluorophenylrhodamines, compared to the "classical" rhodamines carrying 2′-carboxyphenyl substituents.

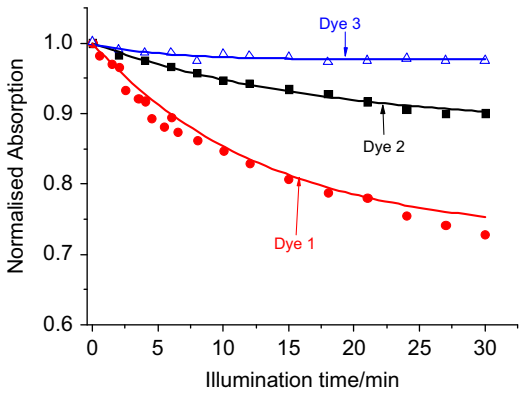

Fig. 6. Photodegradation profiles (approximated with monoexponential decay) of **1–3** in aqueous buffer solution (100 mM; pH=7.5) when illuminated with a 525 nm high-power LED (3 W). The solutions (3 ml) were placed in a glass cuvette and irradiated in a fixed position with respect to the light source. The photodegradation profiles were obtained by monitoring the absorption spectra in the absorption maximum of each dye. Dye concentration was adjusted so that $A_{525}=0.4$ for all dyes.

However, the sensors based on **1** and **2** are still very robust under the employed measurement conditions. In fact, continuous illumination with a standard 5 mm, 525 nm LED over >5 h caused no changes in the fluorescence signal. Note that for practical applications, continuous illumination is often not necessary so that measurement can be carried out for a much longer time before recalibration is required. Indeed, if long-time application and high light densities are required, the photostability of the sensors might become an issue.

3.5. Dually lifetime referenced pH sensor

For practical applications, an optical sensor based on fluorescence intensity requires referencing. One possibility is the combination with a luminescent reference material and interrogation by phase fluorimetry (dual lifetime referencing, DLR) [54,55]. The observed phase shift is then a function of the ratio between luminescence intensity of the fluorescent indicator and the luminescent reference material. Cr(III)-doped Al_2O_3 (ruby) was chosen as a reference material because it is spectrally compatible with the sensor particles and the light source (525 nm LED; Fig. 7A) and features good chemical stability and photostability. A typical measurement with pH-sensitive silica particles as sensitive material is shown in Fig. 7B. The referenced sensor shows excellent response and reversibility.

4. Conclusion

A new class of pH-sensitive rhodamines has been presented. Their pH-sensitivity originates from photoinduced electron transfer (PET) from non-protonated amino groups to the excited chromophore. In respect to synthetic accessibility and performance as pH-indicators, they represent a promising alternative to the pH-sensitive rhodamines employing lactame-formation which have been extensively studied [30–34]. The new dyes are suitable for pH monitoring not only in the dissolved state, but also as indicators in pH sensors. In contrast to the rhodamine bearing a 2,4-dicarboxyphenyl group (dye **3**), the new indicators carry a pentafluorophenyl group which enables facile and effective grafting via "click" chemistry. Furthermore, the sensitive properties of the new indicators are not affected by pH-dependent lactonisation, while almost complete lactonisation in the same environment was detected for **3**. Sensors with covalent indicator linkage

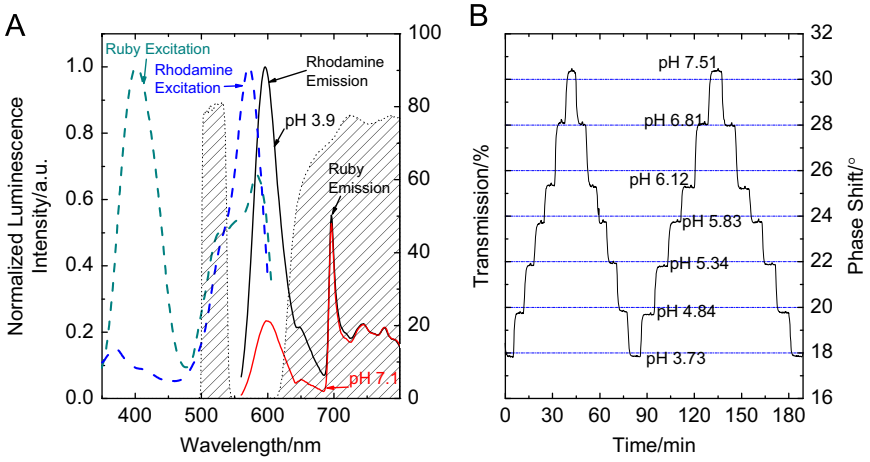

Fig. 7. Properties of the DLR pH sensor (pH-sensitive silica gel beads:ruby 1:6 w/w in a 10 μm thick D4 hydrogel layer): (A) normalised luminescence excitation (dashed lines) of the rhodamine linked to silica gel particles and of ruby; luminescence emission (solid lines) of the DLR sensor at two different pH (both spectra were normalised dividing by the largest intensity count measured at pH 3.9), recorded with a spectrofluorimeter ($\lambda_{EXC}=525$ nm). The transmission of the excitation filter (500–540 nm) and emission filter (>630 nm) are visualised by striped areas. (B) pH-response curve recorded by phase modulation fluorimetry (modulation frequency 550 Hz).

Please cite this article as: D. Aigner, et al., New fluorescent pH sensors based on covalently linkable PET rhodamines, Talanta (2012), http://dx.doi.org/10.1016/j.talanta.2012.05.039

have been successfully prepared based on two matrix materials, silica gel and poly(2-hydroxyethylmethacrylate). Both sensors feature bright fluorescence ($\Phi_F \approx 0.6$) and their sensitive range perfectly matches the pH range of interest for many biotechnological applications (i.e. pH 5–7). They also show good response times, repeatability and long-term stability. For practical applications, a dually lifetime referenced sensor has been presented. Cross-sensitivity to ionic strength causes small to moderate errors (generally 0–0.1, at most 0.2 pH units), provided that the ionic strength is 100–500 mM, which is the case in most biotechnological applications. Although photostability is impaired by the pentafluorophenyl group, it does not compromise the applicability of the sensors under the tested conditions which can be used for a long time without a measurable signal decrease.

Acknowledgement

Financial support from the Austrian Science Fund FWF (Project no. P 21192-N17) and from the Spanish Ministry of Education (Joint Project no. AT2009-0019) is gratefully acknowledged. The authors thank the Institute of Organic Chemistry, Graz University of Technology, particularly Jana Rentner, MSc for kind support in performing LC-MS. Furthermore, we thank Johann Pichler, Institute of Inorganic Chemistry, Graz University of Technology, for acquiring ^{19}F-NMR spectra, as well as Sarah Schiller and Stefan Schobesberger.

Appendix A. Supplementary information

Supplementary data associated with this article can be found in the online version at http://dx.doi.org/10.1016/j.talanta.2012.05.039.

References

[1] S.G. Schulman, S. Chen, F. Bai, M.J.P. Leiner, L. Weis, O.S. Wolfbeis, Anal. Chim. Acta 304 (1995) 165–170.
[2] H.R. Kermis, Y. Kostov, G. Rao, Analyst 128 (2003) 1181–1186.
[3] A. Hakonen, S. Hulth, Anal. Chim. Acta 606 (2008) 63–71.
[4] Y.-H. Chan, C. Wu, F. Ye, Y. Jin, P.B. Smith, D.T. Chiu, Anal. Chem. 83 (2011) 1448–1455.
[5] W. Shi, S. He, M. Wei, D.G. Evans, X. Duan, Adv. Funct. Mater. 20 (2010) 3856–3863.
[6] B.M. Weidgans, C. Krause, I. Klimant, O.S. Wolfbeis, Analyst 129 (2004) 645–650.
[7] A.L. Medina-Castillo, J.F. Fernandez-Sanchez, A. Segura-Carretero, A. Fernandez-Gutierrez, J. Mater. Chem. 21 (2011) 6742–6750.
[8] J.E. Whitaker, R.P. Haugland, F.G. Prendergast, Anal. Biochem. 194 (1991) 330–344.
[9] F. Zhang, Z. Ali, F. Amin, A. Feltz, M. Oheim, Chem. Phys. Chem. 11 (2010) 730–735.
[10] K. Aslan, J.R. Lakowicz, H. Szmacinski, C.D. Geddes, J. Fluoresc. 15 (2005) 37–40.
[11] S.M. Borisov, K. Gatterer, I. Klimant, Analyst 135 (2010) 1711–1717.
[12] M. Beija, C.A.M. Afonso, J.M.G. Martinho, Chem. Soc. Rev. 38 (2009) 2410–2433.
[13] H. Yang, Y. Zhuang, H. Hu, X. Du, C. Zhang, X. Shi, H. Wu, S. Yang, Adv. Funct. Mater. 20 (2010) 1733–1741.
[14] H. Wang, Y. Li, S. Xu, Y. Li, C. Zhou, X. Fei, L. Sun, C. Zhang, Y. Li, Q. Yang, X. Xu, Org. Biomol. Chem. 9 (2011) 2850–2855.
[15] L. Li, X. Tian, G. Zou, Z. Shi, X. Zhang, W. Jin, Anal. Chem. 80 (2008) 3999–4006.
[16] M. Bossi, J. Folling, V.N. Belov, V.P. Boyarskiy, R Medda, A. Egner, C. Eggeling, A. Schönle, S.W. Hell, Nano Lett. 8 (2008) 2463–2468.
[17] E.L. Quitevis, A.H. Marcus, M.D. Fayer, J. Phys. Chem. 97 (1993) 5762–5769.
[18] T.J.V. Prazeres, A. Fedorov, J.M.G. Martinho, J. Phys. Chem. B 108 (2004) 9032–9041.
[19] G.A. Crosby, J.N. Demas, J. Phys. Chem. 75 (1971) 991–1024.
[20] M. Bossi, V.N. Belov, S. Polyakova, S.W. Hell, Angew. Chem. Int. Ed. 45 (2006) 7462–7465.
[21] Y. Shiraishi, R. Miyamoto, X. Zhang, T. Hirai, Org. Lett. 9 (2007) 3921–3924.
[22] J.H. Soh, K.M.K. Swamy, S.K. Kim, S. Kim, S.-H. Lee, J. Yoon, Tetrahedron Lett. 48 (2007) 5966–5969.
[23] Y.-K. Yang, K.-J. Yook, J. Tae, J. Am. Chem. Soc. 127 (2005) 16760–16761.
[24] V. Dujols, F. Ford, A.W. Czarnik, J. Am. Chem. Soc. 119 (1997) 7386–7387.
[25] Y. Xiang, A. Tong, P. Jin, Y. Ju, Org. Lett. 8 (2006) 2863–2866.
[26] Y. Xiang, A. Tong, Org. Lett. 8 (2006) 1549–1552.
[27] J.Y. Kwon, Y.J. Jang, Y.J. Lee, K.M. Kim, M.S. Seo, W. Nam, J. Yoon, J. Am. Chem. Soc. 127 (2005) 10107–10111.
[28] B. Tang, Y. Xing, P. Li, N. Zhang, F. Yu, G. Yang, J. Am. Chem. Soc. 129 (2007) 11666–11667.
[29] H.N. Kim, M.H. Lee, H.J. Kim, J.S. Kim, J Yoon, Chem. Soc. Rev. 37 (2008) 1465–1472.
[30] L. Yuan, W. Lin, Y. Feng, Org. Biomol. Chem. 9 (2011) 1723–1726.
[31] Z. Li, S. Wu, J. Han, S. Han, Analyst 136 (2011) 3698–3706.
[32] S. Wu, Z. Li, J. Han, Chem. Commun. 47 (2011) 11276–11278.
[33] Q.A. Best, R. Xu, M.E. McCarroll, L Wang, D.J. Dyer, Org. Lett. 12 (2010) 3219–3221.
[34] W. Zhang, B. Tang, X. Liu, Y. Liu, K. Xu, J. Ma, L. Tong, G. Yang, Analyst 134 (2009) 367–371.
[35] V. Misra, H. Mishra, H.C. Joshi, T.C. Pant, Sens. Actuators B 63 (2000) 18–23.
[36] V. Misra, H. Mishra, H.C. Joshi, T.C. Pant, Sens. Actuators B 82 (2002) 133–141.
[37] L.M. Daffy, A.P. de Silva, H.Q.M. Gunaratne, C. Huber, P.L.M. Lynch, T. Werner, O.S. Wolfbeis, Chem.–Eur. J. 4 (1998) 1810–1815.
[38] R.A. Bissell, A.P. de Silva, H.Q.N. Gunaratne, P.L.M. Lynch, G.E.M. Maguire, K.R.A.S. Sandanayake, Chem. Soc. Rev. 21 (1992) 187–195.
[39] A.P. de Silva, H.Q.N. Gunaratne, J.-L. Habib-Jiwan, C.P. McCoy, T.E. Rice, J.-P. Soumillion, Angew. Chem. Int. Ed. 34 (1995) 1728–1731.
[40] T. Werner, C. Huber, S. Heinl, M. Kollmannsberger, J. Daub, O.S. Wolfbeis, Fresenius J. Anal. Chem. 359 (1997) 150–154.
[41] K. Kubo, A. Mori, J. Mater. Chem. 15 (2005) 2902–2907.
[42] A.P. de Silva, T.P. Vance, M.E.S. West, G.D. Wright, Org. Biomol. Chem. 6 (2008) 2468–2480.
[43] Y. Koide, Y. Urano, K. Hanaoka, T. Terai, T. Nagano, ACS Chem. Biol. 6 (2011) 600–608.
[44] K. Zhou, Y. Wang, X. Huang, K. Luby-Phelps, B.D. Sumer, J. Gao, Angew. Chem. Int. Ed. 50 (2011) 6109–6114.
[45] C.R. Becer, K. Babiuch, D. Pilz, S. Hornig, T. Heinze, M. Gottschaldt, U.S. Schuberth, Macromolecules 42 (2009) 2387–2394.
[46] C.R. Becer, R. Hoogenboom, U.S. Schubert, Angew. Chem. Int. Ed. 48 (2009) 4900–4908.
[47] D. Samaroo, M. Vinodu, X. Chen, C.M. Drain, J. Comb. Chem. 9 (2007) 998–1011.
[48] G. Vives, C. Giansante, R. Bofinger, G. Raffy, A. Del Guerzo, B. Kauffmann, P. Batat, G. Jonusauskas, N.D. McClenaghan, Chem. Commun. 47 (2011) 10425–10427.
[49] A.C.B. Figueira, K.T. de Oliveira, O.A. Serra, Dyes Pigm. 91 (2011) 383–388.
[50] R.F. Kubin, A.N. Fletcher, J. Lumin. 27 (1982) 455–462.
[51] N. Öztürk, S. Akgöl, M. Arlsoy, A. Denizli, Sep. Purif. Technol. 58 (2007) 83–90.
[52] J. Janata, Anal. Chem. 59 (1987) 1351–1356.
[53] F. Gao, L. Wang, L. Tang, C. Zhu, Microchim. Acta 152 (2005) 131–135.
[54] C. Huber, I. Klimant, C. Krause, O.S. Wolfbeis, Anal. Chem. 73 (2001) 2097–2103.
[55] G. Liebsch, I. Klimant, C. Krause, O.S. Wolfbeis, Anal. Chem. 73 (2001) 4354–4363.

Please cite this article as: D. Aigner, et al., New fluorescent pH sensors based on covalently linkable PET rhodamines, Talanta (2012), http://dx.doi.org/10.1016/j.talanta.2012.05.039